Annals of Nuclear Medicine Vol. 19, No. 3, 217–224, 2005

Use of iodine-123 metaiodobenzylguanidine scintigraphy for the detection of amiodarone induced pulmonary toxicity in a rabbit model: a comparative study with technetium-99m diethyltriaminepenta acetic acid radioaerosol scintigraphy

Gulay DURMUŞ-ALTUN,* Armagan ALTUN,** Ranan Gülhan AKTAS,***
Yavuz Sami SALIHOGLU* and Necmi Omer YİGİTBASI*

*Department of Nuclear Medicine, Faculty of Medicine, Trakya University, Edirne, Turkey
**Department of Cardiology, Faculty of Medicine, Trakya University, Edirne, Turkey
***Department of Histology and Embryology, Faculty of Medicine, Karaelmas University, Zonguldak, Turkey

The purpose of the study was; (i) to determine whether ^{123}I-MIBG scintigraphy is sensitive for detection of amiodarone induced pulmonary toxicity (AIPT) and (ii) to compare it with ^{99m}Tc-DTPA radioaerosol. Twelve white New Zealand rabbit with initial mean body weight 4.24 ± 0.47 g were divided into two groups. AIPT group (n = 7) was administered amiodarone (20 mg/kg BW). The control group (n = 5) received the same amount of 0.9% saline. All animals underwent ^{123}I-MIBG and ^{99m}Tc-DTPA radioaerosol scintigraphy at the end of the treatment period. ^{123}I-MIBG static thorax images were obtained during 10 minutes at 15 minutes and 3-hours after intravenous injection of the radiopharmaceutical. Lung to heart ratios (LHR) and lung to mediastinum ratios (LMR), and retention index (LRI) of ^{123}I-MIBG were determined. Two days after ^{123}I-MIBG scintigraphy, ^{99m}Tc-DTPA radioaerosol scintigraphy was performed, and clearance from the lungs was measured for 10 min (1 min/frame) following termination of inhalation. ^{123}I-MIBG lung retention index (LRI) was significantly higher in the AIPT group than the control (61 ± 4.6 vs. 40 ± 4.5, p = 0.01). Early LHR and LMR were significantly lower in the AIPT group than in the control group (p = 0.04, p = 0.01, respectively), whereas those of late LHR and LMR were not significantly different. $T_{½}$ values of DTPA clearance were significantly increased in AIPT group according to the control group (55 ± 7.2 vs. 86.6 ± 18.5, p = 0.02). ^{123}I-MIBG scintigraphy is a valuable tool for detecting AIPT in a rabbit model. Additionally, ^{99m}Tc-DTPA radioaerosol scintigraphy is an excellent comprehensive investigational tool for detecting AIPT with the added advantage of lower cost.

Key words: amiodarone, pulmonary toxicity, ^{123}I-MIBG, ^{99m}Tc-DTPA radioaerosol, scintigraphy

INTRODUCTION

AMIODARONE (AD) is a useful drug for the treatment of life-threatening cardiac arrhythmia.[1] One of the most serious side effects of AD is lung toxicity, and this limits its utility. In general, the toxicity is characterized by accumulation of phospholipid-rich material resembling surfactant in the lungs, intra-alveolar and interstitial inflammation, and eventually pulmonary fibrosis.[2] The diagnosis of lung toxicity is difficult since the symptoms, clinical findings, and test results are not specific for it.

Technetium-99m-diethyltriaminepenta acetic acid (^{99m}Tc-DTPA) radioaerosol and gallium-67 scintigraphies, the combination of two scintigraphic methods, have been employed for the diagnosis of amiodarone induced pulmonary toxicity (AIPT) in clinical studies.[3–5] Recently, we reported that ^{99m}Tc-DTPA radioaerosol scintigraphy provides an accurate evaluation about stage

Received July 12, 2004, revision accepted January 17, 2005.
For reprint contact: Gulay Durmuş-Altun, M.D., Trakya University, Faculty of Medicine, Department of Nuclear Medicine, 22030 Edirne, TURKEY.
E-mail: gdurmusaltun@trakya.edu.tr

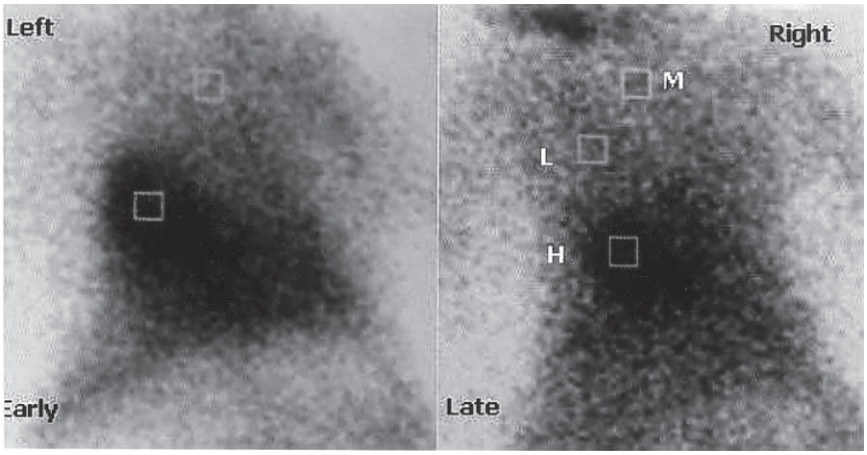

Fig. 1 ^{123}I-MIBG scintigraphy was shown at early (15 minutes) and late (3-hours) phases. Regions of interests from the heart (H), mediastinum (M) and lung area (L) were drawn.

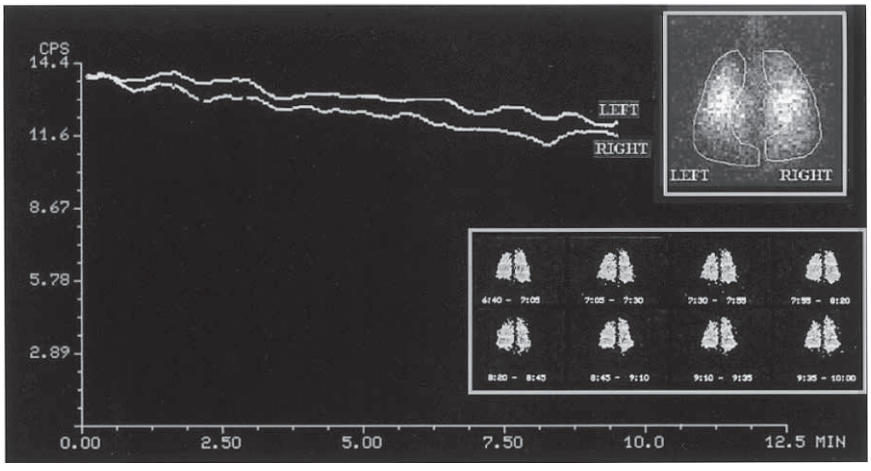

Fig. 2 This figure shows regions of interest from a subject in AIPT group from posterior view of both lungs on ^{99m}Tc-DTPA radioaerosol inhalation lung scintigraphy. The clearance rate ^{99m}Tc-DTPA ($T_{½}$) for right lung is 130 min.

of AIPT.[6] In another experimental study, Capa Kaya et al.[7] suggested that technetium-99m labeled D,L-hexamethylpropylene amine oxime (^{99m}Tc-HMPAO), a cyclic amine, could demonstrate AIPT, and ^{99m}Tc-HMPAO lung uptake was correlated with AD dose.

The lungs are major organs for removal of circulating monoamines, and play a significant role in the inactivation of circulating norepinephrine.[8,9] Radioiodinated metaiodobenzylguanidine (iodine-123 metaiodobenzylguanidine (^{123}I-MIBG)), an analog of guanidine that shares many neuronal transport and storage mechanisms with norepinephrine, has been used to assess the pulmonary endothelial function; it reflects pulmonary endothelial cell injury.[10–14] The purpose of the study was to determine whether ^{123}I-MIBG scintigraphy is sensitive for the detection of AIPT, and to compare the results with ^{99m}Tc-DTPA radioaerosol scintigraphy.

MATERIAL AND METHODS

Animal experiment

Twelve white New Zealand rabbits with initial mean body weight 4.24 ± 0.47 g were divided into two groups. All rabbits were housed individually in standard cages and received food and tap water ad libitum. AD-induced pulmonary toxicity group (n = 7) was administered amiodarone HCl (Cordarone, SANOFI PHARMA, Paris, France) (20 mg/kg BW) intra-peritoneally as a 5% aqueous solution for 6 weeks.[15] The control group (n = 5) received the same amount of 0.9% saline. All animals underwent ^{123}I-MIBG and ^{99m}Tc-DTPA radioaerosol scintigraphy at the end of the treatment period.

Anesthesia was induced by IM administration of 35 mg/kg ketamine and 5 mg/kg xylazine. Experimental animals were euthanized one day after imaging; histo-

Table 1 Detailed results of early- and late-LHR, LMR and lung clearance on ^{123}I-MIBG, and T½ values of lung clearance on ^{99m}Tc-DTPA lung scans in the different study subgroups

	Groups	Mean ± SE	±95% CI	P
^{123}I-MIBG early-LHR	Control	0.62 ± 0.05	0.45–0.79	0.04
	AIPT	0.42 ± 0.07	0.28–0.56	
^{123}I-MIBG early-LMR	Control	1.66 ± 0.21	1.07–2.53	0.01
	AIPT	1.28 ± 0.09	1.04–1.52	
^{123}I-MIBG late-LHR	Control	0.70 ± 0.08	0.50–0.90	NS
	AIPT	0.65 ± 0.06	0.50–0.81	
^{123}I-MIBG late-LMR	Control	1.3 ± 0.193	0.81–1.86	NS
	AIPT	1.54 ± 0.2	0.79–2.54	
^{123}I-MIBG LRI (%)	Control	40 ± 4.5	27–52	0.01
	AIPT	61 ± 4.6	50–72	
^{99m}Tc-DTPA CL (min)	Control	55 ± 7.2	35–75	0.02
	AIPT	86.6 ± 18.5	103–152	

AIPT: Amiodarone induced pulmonary toxicity, LHR: Lung to heart ratios, LMR: Lung to mediastinum ratios, LRI: Lung retention index, CL: Clearance, NS: Non-significant.

pathologic analysis of lungs was then performed. The study protocol was approved by the institutional ethical committee.

^{123}I-MIBG scintigraphy

^{123}I-MIBG (37 MBq) was slowly injected through a secure intravenous line (24F) in an ear marginal vein. Posterior static thorax images in a 128 matrix were obtained during 10 minutes using a low-energy all-purpose collimator, 1.55 zoom factor, 15 minutes and 3-hours after intravenous injection of the radiopharmaceutical. The ^{123}I photopeak was at 159 keV with 20% window set.

Appropriate regions of interest (ROIs) were drawn from the mid-zone of the right lung to prevent scatter from liver activity. Also, ROIs from the heart (H) and mediastinum (M) were drawn (Fig. 1). After correction for the acquisition time and decay, mean counts per pixel were used in the calculations. Lung to heart ratios (LHR) and lung to mediastinum ratios (LMR) were determined. To calculate the lung retention index (LRI) of ^{123}I-MIBG, a previously described formula was used[13]:

Lung retention index of ^{123}I-MIBG
= (delayed uptake/early uptake) × 100

^{99m}Tc-DTPA radioaerosol study

^{99m}Tc-DTPA (CIS, France) was chelated by introducing 30 mCi (1110 MBq) of sodium $^{99m}TcO_4^-$ into 2–3 m*l* of normal saline. ^{99m}Tc-DTPA was placed in the nebulizer reservoir of a commercially available system (Venticis II, CIS, France). Aerosols with a mass median diameter of 0.8 μ were produced with an oxygen in flow of 6 *l*/min. experimental animals inhaled the radioaerosol using a facemask until a count rate of more than 250 cpm, duration time 3 to 6 min, and than were disconnected from the system. The animals were placed over a gamma camera (Orbiter; Siemens Corp., Iselin, NJ, USA) with a low-energy, all-purpose collimator and lung fields were imaged in posterior projection, acquired on a 64 × 64 matrix, 1.55 zoom factor. Clearance from the lungs was measured for 10 min (1 min/frame) following termination of inhalation.

ROIs were drawn around the periphery of the lungs and on the major airways on the first-minute image. To obtain a pure alveolar ROI and to exclude the entire bronchial activity, the outer third of each lung was used as the peripheral lung region. The inner two-thirds of the lung was defined as the central lung region (Fig. 2).

Radioactivity was first corrected for ^{99m}Tc decay and plotted as a logarithmic function of time. An exponential line of best fit was determined by regression analysis, and pulmonary half-life (T½) was calculated from the slope of the line using the formula $N = N0\ e^{-kt}$ (where $N0$ is initial activity in the lung, N is the activity at time t and k is the slope) as an indicator of lung epithelial permeability for right lung. Penetration index (PI) was also calculated by a previously described formula[16] to quantify the distribution of the inhaled aerosol (PI = peripheral total counts/(peripheral total counts + central total counts)).

Histopathologic evaluation

Biopsies from the lungs of the rabbits were pre-fixed in 3% glutaraldehyde in cacodylate buffer and then post-fixed in 1% osmium-tetraoxide in the same buffer. They were dehydrated in alcohol series and embedded in Spurr's resin. Semithin sections, at 0.6 micron thickness, were stained with Toluidine blue. After the examination of semithin sections; ultrathin sections were cut at 200 Angstrom by using UltracutE ultramicrotome. These sections were stained with uranyl acetate and lead citrate. The specimens were examined with a Joel 100 CX electron microscope and pictures were taken.

Table 2 ^{123}I-MIBG LRI and ^{99m}Tc-DTPA aerosol lung clearance values in 12 subjects

Subjects	^{123}I-MIBG Lung retention index (%)	^{99m}Tc-DTPA Lung clearances (min)
AIPT-1	62	95
AIPT-2	60	130
AIPT-3	85	141
AIPT-4	50	121
AIPT-5	62	172
AIPT-6	47	138
AIPT-7	62	98
Control-1	22	73
Control-2	43	47
Control-3	47	72
Control-4	45	39
Control-5	44	44

AIPT: Amiodarone induced pulmonary toxicity.

Table 3 Diagnostic accuracy of scintigraphic indexes for detecting AIPT

	AIPT	Control	
^{123}I-MIBG LRI (%)*			
>52	5	0	$\chi^2 = 6.12$
<52	2	5	p = 0.01
^{99m}Tc-DTPA Lung clearances (min)**			
>75	7	0	$\chi^2 = 12$
<75	0	5	p = 0.0005

AIPT: Amiodarone induced pulmonary toxicity, LRI: Lung retention index, *: Sensitivity = 71%, Specificity = 100%, Overall diagnostic accuracy: 83%, **: Sensitivity = 100%, Specificity = 100%, Overall diagnostic accuracy: 100%.

Statistical analysis

Data are expressed as mean ± SEM. Mann-Whitney U test was employed to compare scintigraphic parameters between the groups. Chi-square test was used for categorical variable. Significance was set at $p < 0.05$.

RESULTS

Scintigraphic indexes were summarized in Table 1. In ^{123}I-MIBG study, early LHR and LMR were significantly lower in the AIPT group than in the control group (p = 0.04, p = 0.01, respectively), whereas that of late LHR and LMR were not significantly different between the two groups. Although ^{123}I-MIBG early LMR and LHR had significantly high values in AIPT group, there was no diagnostic value ^{123}I-MIBG early LMR and LHR for the detection of AIPT in our experimental group. ^{123}I-MIBG LRI was significantly higher in animals with AIPT than control (p = 0.01). ^{123}I-MIBG LRI and ^{99m}Tc-DTPA lung clearance values were shown in Table 2. When the upper limit of 95% CI in control group was accepted as the cut-off value (52%); sensitivity of diagnostic accuracy of ^{123}I-MIBG LRI for detecting AIPT was 71%, specificity of it was 100% and overall diagnostic accuracy was 83% (Table 3). Figure 1 shows early and late ^{123}I-MIBG imaging on an AIPT animal.

^{99m}Tc-DTPA aerosol distributed uniformly throughout the lungs of all animals without central deposition. The mean PI values of control and AIPT were 63 ± 1.6% and 63 ± 2%, respectively. Significantly increased T½ values of DTPA clearance were noted in AIPT group when compared with control group (55 ± 7.2 vs. 86.6 ± 18.5, p = 0.02). When a T½ value of DTPA clearance of 75 min

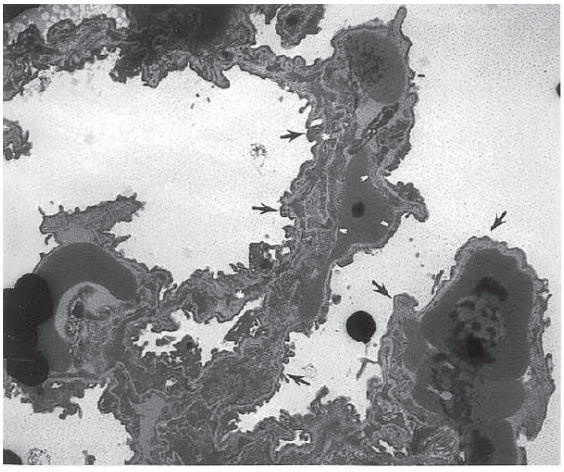

Fig. 3 An electron micrograph from an experimental animal of control group. Type I alveolar cells (*arrows*), endothelial cells (*arrowheads*) and interalveolar septum (*) show normal ultrastructural features. (×4000, Uranyl acetate & Lead citrate)

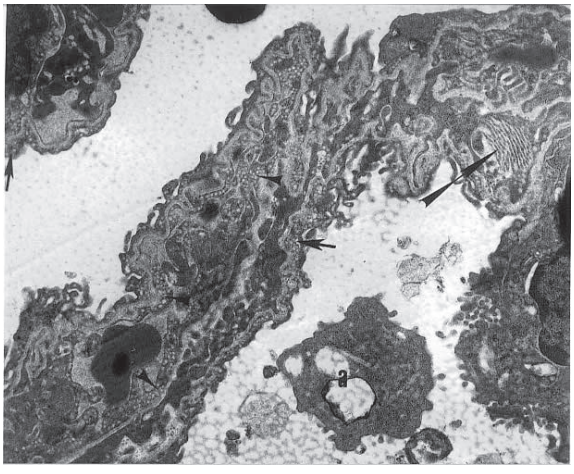

Fig. 4 A micrograph from an experimental animal that has been treated with amiodarone. There is a significant increase at the pinocytotic vesicles in the cytoplasm of either Type I cells (*arrows*) or endothelial cells (*arrowheads*). Note also the striking increase of collagen fibers in interalveolar septum. a: An alveolar macrophage in the alveolar space. (×7500, Uranyl acetate & Lead citrate)

Table 4 The ultrastructural features of AIPT subjects

AIPT subjects	Ultrastructural features
Subject 1	Increased pinocytotic vesicles in Type I alveolar cells
	Increased pinocytotic vesicles in cytoplasm of capillary endothelial cells
	Increased collagen and elastic fibers in interalveolar septum
Subject 2	Increased collagen and elastic fibers in interalveolar septum
	Increased Type II cells and microvilli on the apical surface of Type II cells
	Increased pinocytotic vesicles in cytoplasm of Type II cells
	Decreased lamellar bodies in the cytoplasm of Type II cells
Subject 3	Increased collagen and elastic fibers in interalveolar septum
	Increased pinocytotic vesicles in Type I alveolar cells
Subject 4	Increased collagen and elastic fibers in interalveolar septum
	Increased Type II cells
	Increased pinocytotic vesicles in Type I alveolar cells
Subject 5	Increased collagen and elastic fibers in interalveolar septum
Subject 6	Increased collagen and elastic fibers in interalveolar septum
	Decreased lamellar bodies in the cytoplasm of Type II cells
	Increased Type II cells
	Increased pinocytotic vesicles in Type I alveolar cells
	Increased pinocytotic vesicles in cytoplasm of capillary endothelial cells
Subject 7	Increased collagen and elastic fibers in interalveolar septum

AIPT: Amiodarone induced pulmonary toxicity.

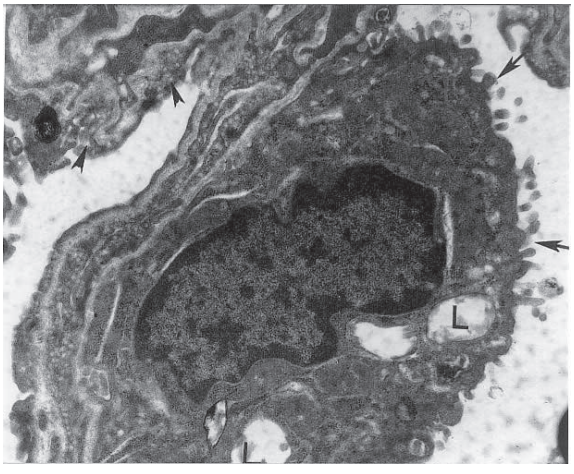

Fig. 5 A micrograph from an animal, which is different from the animal in Figure 5. There are numerous microvilli (*arrows*) on the apical surface of a Type II alveolar cell and only a few lamellar bodies (L) in the cytoplasm. Many pinocytotic vesicles in the endothelial cell are clear. (×5000, Uranyl acetate & Lead citrate)

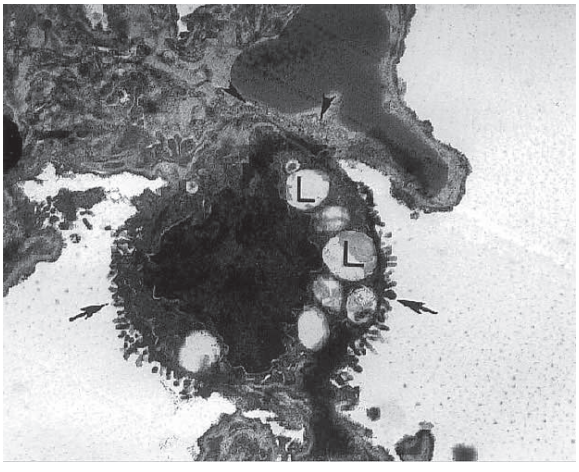

Fig. 6 Another micrograph from another animal. An increase of the microvilli (*arrows*) on the apical surface of Type II cell is clear. There are structurally different lamellar bodies (L) in the cytoplasm of the cell. Note many pinocytotic vesicles in the cytoplasm of the endothelial cell. (×6000, Uranyl acetate & Lead citrate)

(upper limits of 95% CI in control subject) was accepted as the cut-off value, $T_{½}$ values of DTPA clearance of >75 yielded a sensitivity of 100%, a specificity of 100%, and an overall diagnostic accuracy of 100% for detecting AIPT.

The morphologic examination of the lung biopsies showed that Type I alveolar cells, Type II alveolar cells and capillary endothelial cells of rabbits from control group had normal ultrastructural features. The thickness and structure of the fused basal membrane between Type I cells and endotherial cells was normal. There were a few elastic and collagen fibrils in the interalveolar septum (Fig. 4).

After the treatment with AD; there were morphological changes on the lungs of different experimental animals at different level (Table 4). The most significant fine structural change in Type I alveolar cells was the striking increase in pinocytotic vesicles (Figs. 4 and 5). We also observed similar findings in the cytoplasm of endothelial cells (Figs. 4 and 6). An increase in the number of microvilli on the apical surface of Type II cells was evident. The number of lamellar bodies in the cytoplasm

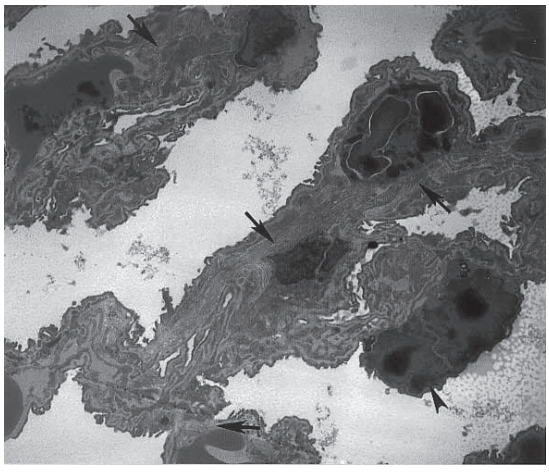

Fig. 7 It is evident that there is a significant increase in the number of collagen fibers (*arrows*). There are also a few cells, which are undergoing necrosis (*arrowheads*). (×3000, Uranyl acetate & Lead citrate)

was decreased and showed morphological changes (Figs. 4 and 6). Another significant finding was an increase of collagen and elastic fibers in interalveolar septum. Some of the alveolar cells contained many lysosomes. It was difficult to recognize the cytoplasmic organelles in some cells, which showed that these cells were undergoing necrosis (Fig. 7).

DISCUSSION

Administration of AD is lifesaving in many conditions for patients with cardiac diseases. However it is associated with serious pulmonary side effects.[1] AIPT is one of the most important examples of drug-induced lung disease by non-cancer chemotherapeutic agents. Patients with AIPT can present with either a chronic disorder that suggests pulmonary fibrosis or a more acute process. Although the risk of a patient developing AIPT increases as the dosage and duration of therapy increase,[17] low-dose therapy is not safe either.[18] Once AIPT has been diagnosed, therapeutic options are limited, but in most cases the disease is reversible if diagnosed at an early stage.[17]

It has been reported that ^{123}I-MIBG has diagnostic value in recognizing minimal endothelial cell lesions.[8,10–13] In our study, significantly decreased ^{123}I-MIBG early LMR and increased ^{123}I-MIBG LRI were observed in AIPT group. In our opinion, these findings could be explained with the morphological changes on the lungs in AIPT group. We observed a striking increase in the number of pinocytotic vesicles in the cytoplasm of endothelial cells. Lung uptake of ^{123}I-MIBG is primarily in endothelial cells, and its lung uptake, as well as its washout, requires normal endothelial cell integrity.[9,11,13] The decrease in this extraction (decreased early LMR and LHR) and slow washout (increased LRI) may simply be linked to endothelial injury. The results of the present study show that ^{123}I-MIBG scintigraphy is a moderately sensitive and highly specific tool for detecting AIPT. To the best of our knowledge, there are no data in the English literature to assess the diagnostic value of ^{123}I-MIBG scintigraphy in subjects with AIPT.

^{99m}Tc-DTPA is deposited in the lining layer of the pulmonary epithelial surface, and transfer of this hydrophilic solute across the alveolar-capillary barrier depends on passive diffusion through the intercellular junctions of the epithelium and endothelium.[19–23] The overall change in alveolar clearance of the solute is determined by the interplay of the surface area for transfer, the concentration gradient across the alveolar-capillary membrane, and the distance of the diffusion pathway of the solute.[21] Interstitial pulmonary fibrosis is caused by an overaggressive repair process, which is accompanied by the presence of a large number of fibroblasts, an increase in absolute collagen levels, a thickening of the basement membrane, and an abnormal ultrastructural appearance. Our study showed significant prolongation of ^{99m}Tc-DTPA radioaerosol lung clearance in AIPT subjects. Another significant morphologic finding of our study was an increase in collagen and elastic fibers in interalveolar septum in the AIPT group. Degeneration of alveolar-capillary membrane may retard alveolar DTPA clearance by increasing the diffusion distance of the solute.[23–25] In contrast to our findings, in clinical studies, Terra-Filho et al.[5] found no difference in ^{99m}Tc-DTPA lung clearance between patients receiving amiodarone and a normal group, while Dirlik et al.[3] found accelerated lung clearance in patients with AIPT. In our previous study, we reported that ^{99m}Tc-DTPA radioaerosol inhalation lung scintigraphy was a sensitive tool for the detection of different histopathologic stages and demonstrated the alteration of lung epithelial permeability, as measured by ^{99m}Tc-DTPA radioaerosol lung scintigraphy in AIPT with and without fibrosis. All specimens in the AIPT group had lung fibrosis and this explains the significant prolongation of ^{99m}Tc-DTPA radioaerosol lung clearance. The present study also shows that ^{99m}Tc-DTPA radioaerosol lung clearance has excellent sensitivity, specificity and diagnostic accuracy.

In summary; the main findings in this study are (i) ^{123}I-MIBG scintigraphy is sensitive for detection of AIPT; and (ii) ^{99m}Tc-DTPA aerosol scintigraphy has excellent diagnostic value for the detection of AIPT in a rabbit model. To the best of our knowledge, there are no data in the English literature to compare the diagnostic value of ^{99m}Tc-DTPA aerosol scintigraphy and ^{123}I-MIBG scintigraphy by using i.v. injection on lung injury. Antonelli Incalzi et al.[26] used ventilatory scintigraphies with ^{123}I-MIBG and ^{99m}Tc-DTPA to assess both bronchopulmonary neuroadrenergic innervation and permeability of the alveolar-capillary barrier to water-soluble tracers in type-1 diabetes mellitus. They also reported that ^{123}I-MIBG

clearance was independent of ^{99m}Tc-DTPA clearance. Previous studies reported that ^{123}I-MIBG scintigraphy is a sensitive tool for detecting pulmonary endothelial cell injury.[8,10–13] Nevertheless, our results showed that ^{99m}Tc-DTPA aerosol scintigraphy is more sensitive than ^{123}I-MIBG scintigraphy for the detection of AIPT. Our previous data also shown that ^{99m}Tc-DTPA radioaerosol lung clearance discriminates the different tissue manifestations—interstitial pneumonia or fibrosis—of AIPT.[6] The measurement of ^{99m}Tc-DTPA lung clearance is a sensitive, low cost and noninvasive method to evaluate acute as well as chronic changes in lung permeability. In the present study, all subjects were detected by using ^{99m}Tc-DTPA lung clearance scintigraphy, but not ^{123}I-MIBG lung scintigraphy. This lower sensitivity may be attributed to our animal model, all subjects are AIPT with fibrosis, and ^{123}I-MIBG might have different tracer kinetics on fibrosis than interstitial pneumonia. This issue warrants further investigation, and additional studies are required to clarify the role of ^{123}I-MIBG scintigraphy for detecting AIPT in different study groups, particularly including interstitial pneumonia and clinical cases.

CONCLUSION

The current study shows that ^{123}I-MIBG scintigraphy, is a valuable tool for detecting AIPT in a rabbit model. ^{99m}Tc-DTPA radioaerosol scintigraphy is an excellent comprehensive investigational tool for detecting AIPT with the added advantage of lower cost. Our study suggests the feasibility and potential diagnostic value of ^{99m}Tc-DTPA lung clearance in AIPT, and it could be become the first choice imaging tool for the diagnosis of AIPT.

REFERENCES

1. Desai AD, Chun S, Sung RJ. The role of intravenous amiodarone in the management of cardiac arrhythmias. *Ann Intern Med* 1997; 127: 294–303.
2. Reasor MJ, Kacew S. An evaluation of possible mechanisms underlying amiodarone-induced pulmonary toxicity. *Proc Soc Exp Biol Med* 1996; 212: 297–304.
3. Dirlik A, Erinc R, Ozcan Z, Atasever A, Bacakoglu F, Nalbantgil S, et al. Technetium-99m-DTPA aerosol scintigraphy in amiodarone induced pulmonary toxicity in comparison with Ga-67 scintigraphy. *Ann Nucl Med* 2002; 16: 477–481.
4. Zhu YY, Botvinick E, Dae M, Golden J, Hattner R, Scheinman M. Gallium lung scintigraphy in amiodarone pulmonary toxicity. *Chest* 1988; 93: 1126–1131.
5. Terra-Filho M, Vargas FS, Meneguetti JC, Soares Junior J, Cukire A, Teixeira LR, et al. Pulmonary clearance of technetium 99m diethylene triamine penta-acetic acid aerosol in patients with amiodarone pneumonitis. *Eur J Nucl Med* 1990; 17: 334–337.
6. Durmus Altun G, Altun A, Salihoglu YS, Altaner S, Berkarda S, Ozbay G. Value of technetium-99m diethyltriamine pentaaceticacid radioaerosol inhalation lung scintigraphy for the stage of amiodarone-induced pulmonary toxicity. *Int J Cardiol* 2004; 95: 193–197.
7. Capa Kaya G, Bekis R, Kirimca F, Ertay T, Kargi A, Gure A, et al. Use of technetium-99m HMPAO scintigraphy for the detection of amiodarone lung toxicity in a rabbit model. *Eur J Nucl Med* 2001; 28: 346–350.
8. Sole MJ, Drobac M, Schwartz L, Hussain MN, Vaughan-Neil EF. The extraction of circulating catecholamines by the lungs in normal man and in patients with pulmonary hypertension. *Circulation* 1979; 60: 160–163.
9. Glowniak JV, Wilson RA, Joyce ME, Turner FE. Evaluation of metaiodobenzylguanidine heart and lung extraction fraction by first-pass analysis in pigs. *J Nucl Med* 1992; 33: 716–723.
10. Slosman DO, Polla BS, Donath A. ^{123}I-MIBG pulmonary removal: a biochemical marker of minimal lung endothelial cell lesions. *Eur J Nucl Med* 1990; 16: 633–637.
11. Giordano A, Calcagni ML, Rossi B, Fuso L, Accardo D, Valente S, et al. Potential use of iodine-123 metaiodobenzylguanidine radioaerosol as a marker of pulmonary neuroadrenergic function. *Eur J Nucl Med* 1997; 24: 52–58.
12. Unlu M, Inanir S. Prolonged lung retention of iodine-123-MIBG in diabetic patients. *J Nucl Med* 1998; 39: 116–118.
13. Unlu M, Akincioglu C, Yamac K, Onder M. Pulmonary involvement in Behçet's disease: evaluation of ^{123}I-MIBG retention. *Nucl Med Commun* 2001; 22: 1083–1088.
14. Arao T, Takabatake N, Sata M, Abe S, Shibata Y, Honma T, et al. *In Vivo* Evidence of Endothelial Injury in Chronic Obstructive Pulmonary Disease by Lung Scintigraphic Assessment of (123)I-Metaiodobenzylguanidine. *J Nucl Med* 2003; 44: 1747–1754.
15. Kannan R, Miller S, Singh BN. Tissue uptake and metabolism of amiodarone after chronic administration in rabbits. *Drug Metab Dispos* 1985; 13: 646–650.
16. Capa Kaya G, Durak H, Yamez B, Turhal U, Ozdogan O, Sayit E, et al. Technetium-99m DTPA inhalation scintigraphy in patients treated with fluoxetine and maprotiline: preliminary results. *Eur J Nucl Med* 2000; 27: 1402–1404.
17. Limper AH, Rosenow III EC. Drug-induced pulmonary disease. In: *Text Book of Respiratory Medicine*. Murray JF, Nadel JA (eds), 3rd ed. Philadelphia; W.B. Saunders Company, 2000: 1971–1984.
18. Ott MC, Khoor A, Leventhal JP, Paterick TE, Burger CD. Pulmonary toxicity in patients receiving low-dose amiodarone. *Chest* 2003; 123: 646–651.
19. Coates G, O'Brodovich H. Measurement of pulmonary epithelial permeability with ^{99m}Tc-DTPA aerosol. *Semin Nucl Med* 1986; 16: 275–284.
20. Line BR. Scintigraphic studies of inflammation in diffuse lung disease. *Radiol Clin North Am* 1991; 29: 1095–1114.
21. O'Doherty MJ, Peters AM. Pulmonary technetium-99m diethylene triamine penta-acetic acid aerosol clearance as an index of lung injury. *Eur J Nucl Med* 1997; 24: 81–87.
22. Effros RM, Mason GR. Measurement of pulmonary epithelial permeability *in vivo*. *Am Rev Respir Dis* 1983; 127 (Suppl): S59–65.
23. Susskind H. Technetium-99m-DTPA aerosol to measure alveolar-capillary membrane permeability. *J Nucl Med* 1994; 35: 207–209.

24. Groeneveld AB. Radionuclide assessment of pulmonary microvascular permeability. *Eur J Nucl Med* 1997; 24: 449–461.
25. Suga K, Alderson PO, Mitra A, Domingues C, Rescigno J, Smith LG, et al. Early retardation of ^{99m}Tc-DTPA radioaerosol transalveolar clearance in irradiated canine lung. *J Nucl Med* 2001; 42: 292–299.
26. Antonelli Incalzi R, Fuso L, Giordano A, Pitocco D, Maiolo C, Calcagni ML, et al. Neuroadrenergic denervation of the lung in type I diabetes mellitus complicated by autonomic neuropathy. *Chest* 2002; 121: 443–451.